STUDY ON RADAR CROSS SECTION FOR FLYING-WING UNMANNED AERIAL VEHICLE WITH CLOSE FORMATION FLIGHT

He Xiaoxiao*
***Aviation Industry Development Research Center of China**

Keywords: *Radar Signature, Formation Flight, Flying Wing*

Abstract

In this paper one typical stealth aircraft concepts (flying-wing) were designed. Then three different echelon formation and wedge formation with the same flying-wing aircraft were created. Based on multilevel fast multipole algorithm (MLFMA), the vertical polarization transmitting/vertical polarization receiving and horizontal polarization transmitting/horizontal polarization receiving radar cross section (VV RCS and HH RCS) characteristics were simulated with frequency of 0.1 GHz. The influences and mechanisms of close formation on electromagnetic scattering characteristics were investigated. The results show that, for the flying wing aircraft and formation, the HH RCS of this frequency range is higher than the VV RCS in most cases. The HH and VV RCS of formation is not just 4 times the RCS of one flying wing aircraft. Changes in formation have little effect on RCS, the spikes are mainly caused by the leading and trailing edge of the sweep wing.

1 Introduction

Multiple unmanned aerial vehicle (UAV) formation has gradually become the main air combat style of major military powers, and it will be used in warfare soon.[1] The United States Department of defense has tested "Perdix" UAV formation several times since September 2014. In October 25, 2016, two F/A-18 carried 103 “Perdix” UAVs, completed continuous air drop tests, creating the largest flight formation record of military UAVs.[2] With the development of next generation surface-to-air missile and anti-stealth radar technology, the new distributed combat system of system of UAVs can adapt better to complex and fierce battle environment. At present, the design of stealth aircraft is not aimed at the flight formation stealth, so this may have a major impact on stealth of a flight formation.[3-4] This paper studies the influence of formation on the stealth of multiple aircraft and tries to give some suggestions for stealth design of UAV.

2 Geometrical configurations

2.1 Flying-wing configuration

One typical stealth aircraft concepts (flying-wing) were designed. A flying wing aircraft appearance is smooth and simple, is conducive to the drawing surface mesh. Figure 1 shows the geometry dimension of flying-wing configuration. As can be seen in the figure, the model is the actual complete flying-wing aircraft model. The whole wing span is 21.6 m, the length of the central fuselage is 7.8 m, and the straight wing chord length is 2.4 m, the sweep angle is 35°.

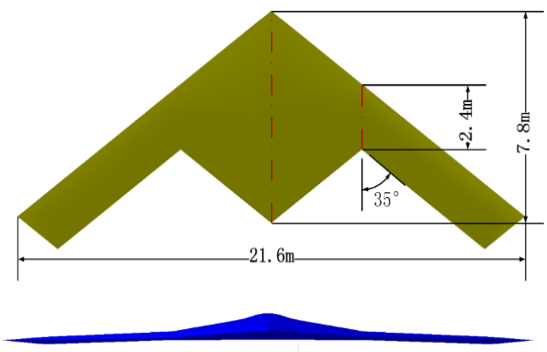

Fig. 1 Flying wing aircraft geometry dimension

2.2 Three Formation

To save computing resources and time, the formation scale will be limited. This paper simplifies the formation of complex swarm formation flights and uses four aircraft formations as the research object. By adjusting the space position among four aircraft, the RCS of each formation is calculated and the stealth characteristics of different formations are analyzed. The three formations are shown in Figure 2, F_1, F_2 and F_3. In F_1, the four aircraft were in the right echelon team, with a vertical interval of 12 meters and a horizontal interval of 12 meters. Four aircraft were on the same height level. In F_2, the four aircraft were in the right wedge team, with a vertical interval of 12 meters and a horizontal interval of 12 meters. Four aircraft were on the same height level. Compared to F_2, the height difference between four aircraft in F_3 is incremented by 5 meters.

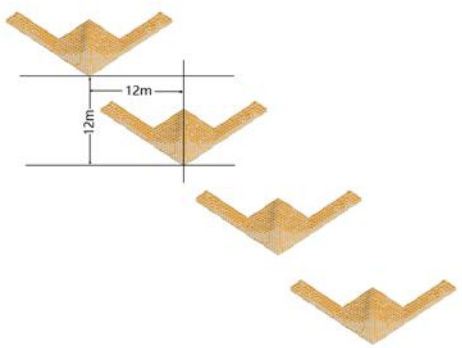

(a) Formation 1(F_1)

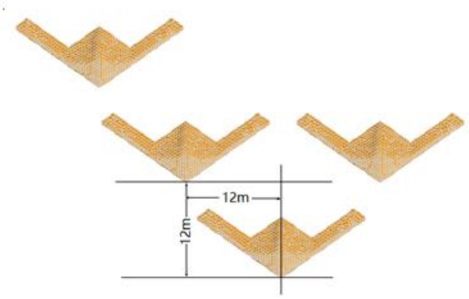

(b) Formation 2(F_2)

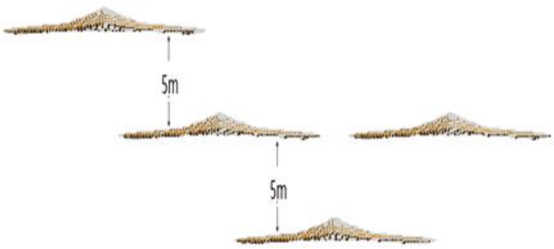

(c) Formation 3(F_3)

Fig. 2 Formation geometry dimension

3 Computation concept and validation

To validate the numerical simulation method, it is necessary to do an electromagnetic test of the scaled aircraft model in the anechoic chamber or to find reliable experimental results. At present the main numerical simulation methods of aircraft RCS are high frequency algorithms.[7-9] The major advantages of these algorithms are low time consumption and low memory requirement. The down side is that they cannot precisely simulate the target's surface current. The high frequency algorithms are also not suitable to solve complex scattering targets like aircraft surface structure gaps and steps.[10] The Method of Moments (MOM) has high calculation accuracy but requires high memory level and has low time efficiency.[11-12] The MOM cannot simulate large scattered like aircraft. The multilevel fast multipole algorithm (MLFMA) is a high efficiency and precision-controlled algorithm. Owing to high precision and efficiency, the MLFMA has found wide applications in aircraft RCS calculations in recent year. [13-17]In this paper the MLFMA was used to numerically simulate the RCS characteristics of the aircraft models.

After electromagnetic testing and numerical simulation of the flying wing by MLFMA, the simulated RCS spike and curve trend is consistent with that determined by the electromagnetic test. All of these prove the simulation results of numerical methods and aircraft RCS characteristics in this study.

4 Presentation of results

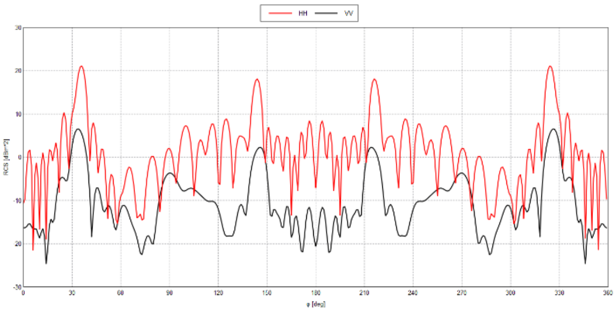

(a) The HH and VV RCS curves of flying wing aircraft

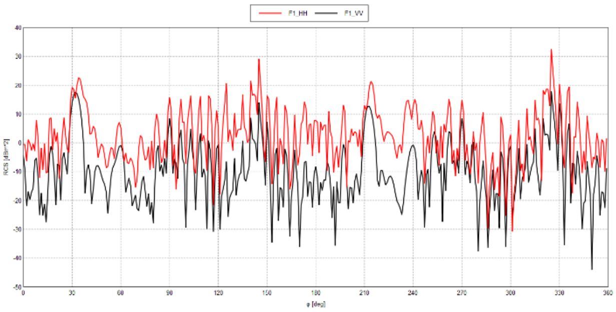

(b) The HH and VV RCS curves of formation 1

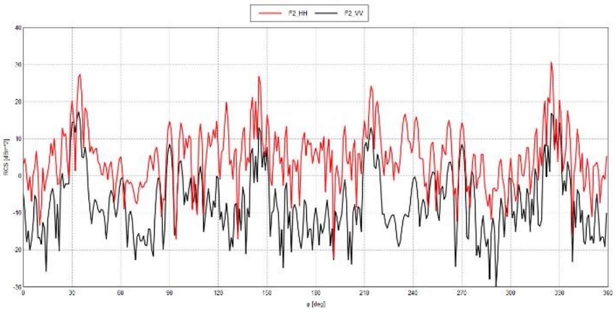

(c) The HH and VV RCS curves of formation 2

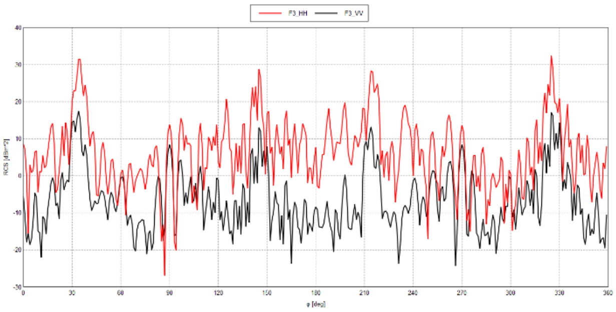

(d) The HH and VV RCS curves of formation 3

Fig. 3 VV and HH RCS characteristics of one aircraft and formation

Figure 3 shows the HH and VV RCS characteristics of the one flying wing aircraft and the different formation. When the radiation frequency is 100 MHz, the RCS curve fluctuates little along the circumferential direction, no significant RCS spike appears. For the one flying wing aircraft, the HH RCS of this frequency range is higher than the VV RCS. It is also a common characteristic for the RCS curves of F_1, F_2 and F_3 model.

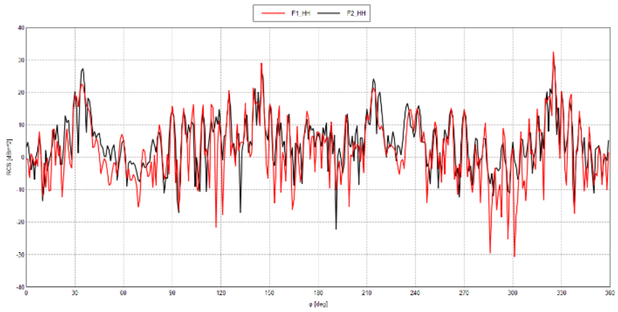

(a) The HH RCS curves of F_1 and F_2

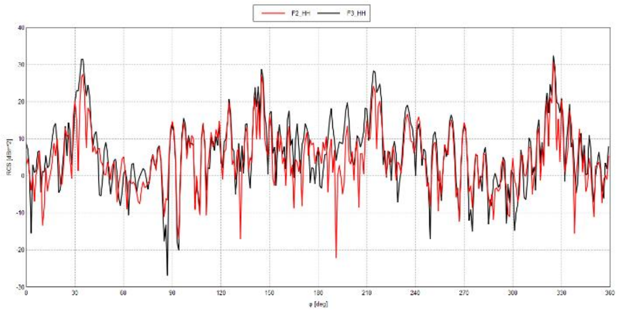

(b) The HH RCS curves of F_2 and F_3

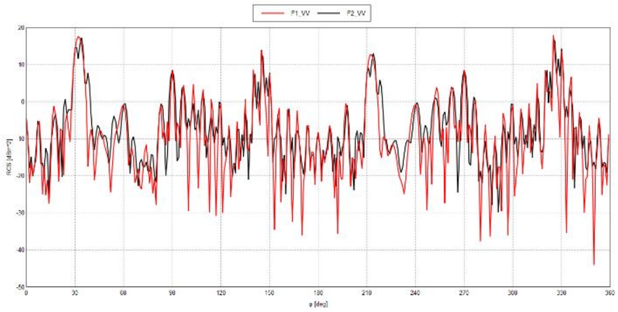

(c) The VV RCS curves of F_1 and F_2

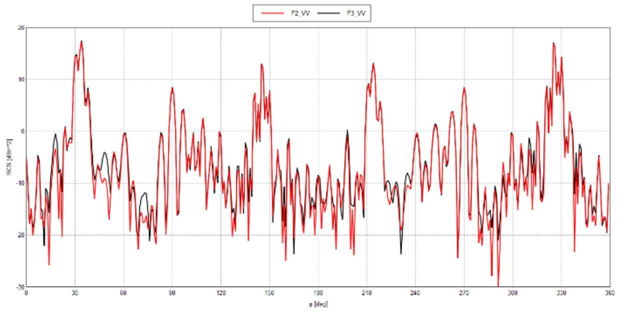

(d) The VV RCS curves of F_2 and F_3

Fig. 4 VV and HH RCS comparison of F_1, F_2 and F_3

In Figure 4, the HH and VV RCS of F_1, F_2 and F_3 formations are different but the trend of curve is close. For both the vertical polarization radiation and horizontal polarization, the RCS spikes located at azimuth 35° and 145° position. These spikes are mainly caused by the leading and trailing edge of the sweep wing.

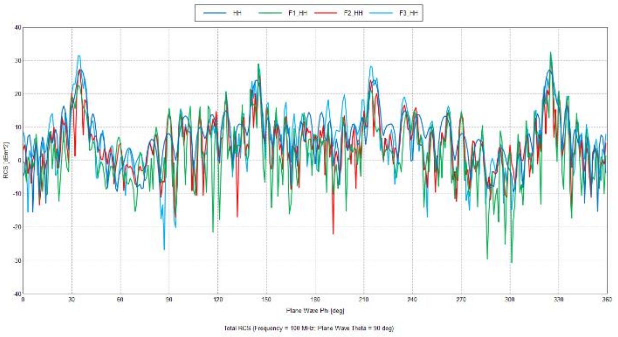

(a) The HH RCS curves of 4*one aircraft

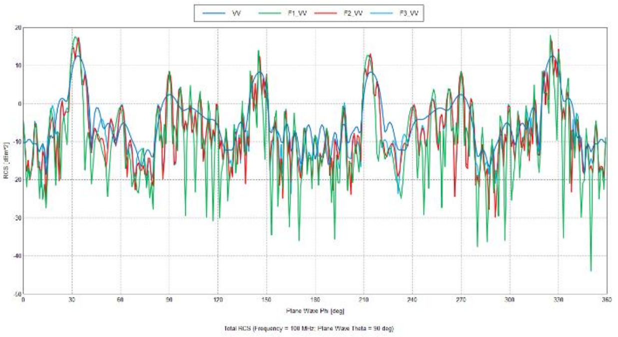

(b) The VV RCS curves of 4*one aircraft

Fig. 5 VV and HH RCS comparison of 4*one aircraft and formation

As can be seen from Figure 5, when the HH and VV RCS of a flying wing aircraft is quadrupled, it is very close to the HH and VV RCS of the flying wing formation. Due to the coupling scattering between aircraft, RCS of the formation is not four times that of a single aircraft RCS. The RCS spikes position is the same position, but the RCS curve is not coincident.

Tab. 1 VV RCS of azimuth angle(m^2)

Average VV RCS	F_1(m^2)	F_2(m^2)	F_3(m^2)
330°-30°	0.8859	0.9534	0.9950
30°-150°	2.6874	2.4575	2.5526
150°-210°	0.3179	0.3364	0.3639
210°-330°	1.9806	2.3277	2.3949

Tab. 2 HH RCS of azimuth angle(m^2)

Average HH RCS	F_1(m^2)	F_2(m^2)	F_3(m^2)
330°-30°	7.0060	7.3129	9.0305
30°-150°	22.3370	28.2605	58.2480
150°-210°	6.0619	6.2654	15.9408
210°-330°	28.9909	29.6185	55.8325

As can be seen from Table 1 and Table 2, at radiation frequency of 0.1 GHz, the average value of HH RCS of formation in all azimuth angle is bigger than VV RSC. The average HH and VV RCS of the echelon formation(F_1) is better than that of the wedge formation(F_2). At the same altitude, F_1 is more dispersed than F_2. Due to the effect of coupled scattering, the stealth effect of F_1 is better. Since F_3 increased the height difference between aircrafts based on F_2, this may be increased coupling scattering between aircraft. Differences in altitude between aircraft may aggravate the effects of coupling scattering.

5 Conclusions

In the present study, the influence of aircraft formation distribution on the stealth performance was investigated through the MLFMA numerical simulation. The results are summarized as follows:

(1) For the flying wing aircraft and flying formation, the HH RCS of this frequency range is higher than the VV RCS in most cases.

(2) The HH and VV RCS of formation is not 4 times the RCS of one flying wing aircraft, but the difference is not significant.

(3) Echelons formations have a slight advantage over wedge formations but the different formations basically have no influence on VV and HH RCS, the spikes are mainly caused by the leading and trailing edge of the sweep wing.

References

[1] Unmanned Aerial Vehicles: Robotic Air Warfare 1917–2007, By Steven Zaloga, Osprey Publishing, 19 July 2011, page 22

[2] "DoD ramps micro-drones after successful 'swarm' test". www.defensesystems.com. Defense Systems. Retrieved 3 September 2017.
[3] Cambone S. Unmanned Aircraft Systems Roadmap 2005-2030[J]. United States.dept.of Defense.office of the Secretary of Defense, 2005.
[4] Parunak H V, Purcell M, O'Connell R. Digital Pheromones for Autonomous Coordination of Swarming UAV's[C]// Uav Conference. 2002:2002-3446.
[5] Ruan Y Z. *Radar cross section and stealth technology.* Beijing: National Defense Industry Press, , 1998. p. 11-12.[Chinese]
[6] Yue KZ, Sun C, Ji JJ. Numerical simulation on the stealth characteristics of twin-vertical-tails for fighter. *J Journal of Beijing University of Aeronautics and Astronautics* 2014; 40(2): 160-5[Chinese].
[7] Chen S, Yue K, Hu B, et al. Numerical Simulation on the Radar Cross Section of Variable-Sweep Wing Aircraft. *J Journal of Aerospace Technology and Management*, 2015;7(2): 170-8.
[8] Song J M, Lu C C, Chew W C. Multilevel fast multipole algorithm for electromagnetic scattering by large complex objects. IEEE Transactions on Antennas and Propagation 1997; 45(10): 1488-93.
[9] Knott E F. A progression of high-frequency RCS prediction techniques. *J Proceedings of the IEEE* 1985; 73(2): 252-264.
[10] Senior T, Volakis J L. Scattering by gaps and cracks. *J Antennas and Propagation, IEEE Transactions* 1989; 37(6): 744-50.
[11] Wang J J H. *Generalized moment methods in electromagnetics: formulation and computer solution of integral equations*. NewYork: Wiley-Interscience, 1991.
[12] Gao ZH, Wang ML. An efficient algorithm for calculating aircraft RCS based on the geometrical characteristics. J Chinese Journal of Aeronautics 2008; 21(4): 296-303.
[13] Liu ZH, Huang PL, Gao X, et al. Multi-frequency RCS reduction characteristics of shape stealth with MLFMA with improved MMN. *J Chinese journal of aeronautics* 2010; 23(3): 327-33.
[14] Rao S M, Wilton D R, Glisson A W. Electromagnetic scattering by surfaces of arbitrary shape. *J Antennas and Propagation, IEEE Transactions* 1982;30(3): 409-18.
[15] Cui T J, Chew W C, Chen G, et al. Efficient MLFMA, RPFMA, and FAFFA algorithms for EM scattering by very large structures. IEEE Transactions on Antennas and propagation 2004; 52(3): 759-770.
[16] Liu Z H, Wu Z, Zhou J, et al. Improving multilevel fast multipole algorithm. *J* Acta Aeronautica et Astronautica Sinica, 2008, 29(5): 1180-5.
[17] LIU Z, TIAN Q, ZHOU J, et al. Analysis of scattering characteristics of aircrafts based on MLFMA. J Journal of Hefei University of Technology (Natural Science), 2008:31(12): 2044-8[Chinese].

Copyright Statement